Clays and Clay Minerals, Vol. 38, No. 1, 33–46, 1990.

MORPHOLOGICAL, CHEMICAL, AND ISOTOPIC EVIDENCE FOR AN EARLY DIAGENETIC EVOLUTION OF DETRITAL SMECTITE IN MARINE SEDIMENTS

NORBERT CLAUER,[1] JAMES R. O'NEIL,[2] CHANTAL BONNOT-COURTOIS,[3] AND THIERRY HOLTZAPFFEL[4]

[1] Centre de Géochimie de la Surface, 67084 Strasbourg, France

[2] Department of Geological Sciences, University of Michigan, Ann Arbor, Michigan 48109

[3] Laboratoire de Géomorphologie, 35800 Dinard, France

[4] Laboratoire de Géologie, Université d'Angers, 49045 Angers, France

Abstract—Mineralogical (XRD), morphological (transmission electron microscopy), chemical (major, rare-earth elements, and scanning-transmission electron microscopy), and isotope (Sr, O, H) measurements were made of marine detrital smectite from shales to study their reactions during early diagenesis. Albian, Aptian, and Palaeogene smectite samples were selected from Deep Sea Drilling Project drill cores taken in the Atlantic Ocean and from outcrops and drill cores from Belgium and northern France. Detrital, flake-like smectite particles seem to have adapted to their depositional environment by isochemical dissolution and subsequent crystallization of authigenic, lath-like particles. The major-element and rare-earth element compositions of both types of particles are similar. The Sr isotope chemistry suggests that the dissolution-crystallization process occurred soon after deposition in an almost closed chemical system. Except for slight changes in the amount of Fe and the oxygen isotope composition, the reaction took place without noticeable chemical exchange with the interstitial or marine environment. Such closed-system recrystallization of clay minerals may be a common diagenetic process if the water/rock ratio is small, as in shales.

Résumé—Une étude minéralogique (diffraction des rayons X), morphologique (éléments majeurs et terres rares, microsonde électronique et microscope électronique à balayage et à transmission), et isotopique (Sr, O, H) a été réalisée sur des smectites-détritiques marines d'argilites pour éxaminer leur évolution diagénétique précoce. Des échantillons albo-aptiens et paléogènes ont sélectionnés de carottes de forages DSDP de l'Océan Atlantique et d'affleurements et de carottes de sondages du nord de la France et de la Belgique.

Les particules de smectites détritiques ont une forme de flocons, et semblent s'adapter à leur environnement de dépôt par dissolution isochimique et cristallisation de lattes authigènes. Les compositions chimiques en éléments majeurs et en terres rares sont très voisines dans les deux types de particules. La géochimie isotopique du Sr suggère que le processus de dissolution-cristallisation a eu lieu rapidement après la sédimentation dans un système chimique pratiquement fermé. A part quelques modifications mineures dans les teneurs en Fe et les compositions isotopiques de l'oxygène, la réaction a eu lieu sans intervention chimique visible de l'environnement interstitiel ou marin. Un tel phénomène de recristallisation des minéraux argileux dans un système chimique clos pourrait être un mécanisme diagénétique commun quand le rapport eau/roche est faible comme c'est le cas dans les shales.

Key Words—Chemical composition, Diagenesis, Isotopic composition, Morphology, Smectite, Transmission electron microscopy, X-ray powder diffraction.

INTRODUCTION

Since the work of Biscaye (1965) and earlier studies, clay minerals in Recent sediments in the Atlantic Ocean have been considered to be mainly of detrital origin (Chamley, 1979; Grousset, 1983), except for those in volcano-sedimentary sequences (Chamley and Bonnot-Courtois, 1981) and in material near hydrothermal effusive structures (Desprairies *et al.*, 1984). Strontium (Dasch, 1969) and oxygen (Savin and Epstein, 1970a, 1970b) isotope data support such interpretation. In older Atlantic sediments, these clay fractions may contain as much as 95% smectite and, because of their assumed pedogenic origin, they have been often used for paleogeographic reconstructions (Chamley and Debrabant, 1982).

Recent smectite of the Pacific Ocean may be of authigenic origin (Hoffert, 1980). After deposition, this smectite can interact with its interstitial environment to produce lath-type particles (Clauer *et al.*, 1982). Alteration and authigenesis were followed by analyses of the $^{87}Sr/^{86}Sr$ ratio of the smectite fractions, which indicated a transfer of radiogenic ^{87}Sr from solid particles to the aqueous environment. Clauer *et al.* (1984) re-

Copyright © 1990, The Clay Minerals Society

https://doi.org/10.1346/CCMN.1990.0380105 Published online by Cambridge University Press

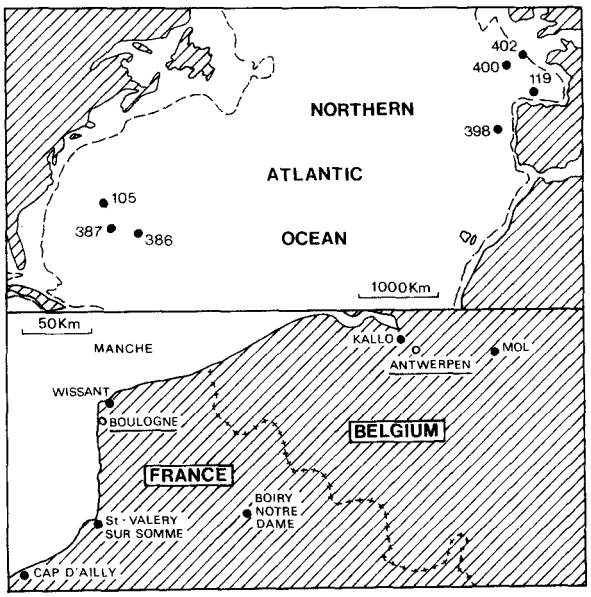

Figure 1. Upper: Location of the Deep Sea Drilling Project bore-cores sampled in the study. Lower: Location of the outcrops in northern France and the bore-holes in Belgium of equivalent on-shore samples.

ported also evidence for morphological modifications of detrital smectite particles, which was accompanied by a loss of radiogenic ^{87}Sr and ^{40}Ar and a change in the chemistry of the particles. These results suggest a tendency towards a chemical equilibrium with the depositional environment.

Because of its potential to equilibrate with the interstitial environment, smectite was investigated in detail in the present study, building on the previous studies. The techniques employed included morphological observations by optical microscopy and transmission electron microscopy (TEM); mineralogical study by X-ray powder diffraction (XRD); chemical analyses by atomic absorption, neutron activation, electron microprobe, scanning-transmission electron microscopy (STEM); and stable and radiogenic isotopic determinations. The aims of the present study were (1) to describe the alteration of the detrital smectite particles, (2) to provide a quantitative measure of the extent of these modifications, and (3) to determine the environment and timing of these modifications.

SAMPLE DESCRIPTION AND METHODS

Smectite is very abundant in Albian, Aptian, and Palaeogene sedimentary sequences of the northern Atlantic Ocean. During late Cretaceous time, when this ocean was forming, sediments were deposited under reducing conditions and became black shales (Arthur, 1979; Cook, 1982). During Palaeogene time, enhanced bottom currents produced oxidizing conditions, which favored deposition of silty claystones containing centimeter-thick chert-rich beds. Such sequences are known elsewhere (Leclaire, 1974; Nathan and Flexer, 1977), and the occurrence of cherty horizons, clinoptilolite, and palygorskite-type clays are thought to be records of the influence of open sea-water.

Ninety-three samples were studied, of which 51 were taken from seven bore-holes (105, 109, 386, 387, 398, 400, and 402) drilled during five Deep Sea Drilling Project legs (11, 12, 43, 47, and 48). Forty-two additional samples were collected from outcrops in northern France or from drill cores in Belgium (Figure 1). All these samples are from the same stratigraphic horizons and are of marine origin. Precise descriptions and locations are available elsewhere (Holtzapffel, 1983), as is a description of the sedimentation conditions (Holtzapffel *et al.*, 1985).

Smear slides and randomly oriented powders were made of all clay-size fractions <2 μm after standard separations had been made by sedimentation in distilled water and were analyzed by XRD. For most samples, no prelimimary crushing was necessary. If necessary, carbonates were removed with 0.2 N HCl. Twenty-six samples having the greatest smectite contents were selected from the XRD data (Table 1). Microscopic observations of the grain sizes, mineral point counts, and Ca and organic-C determinations were also made on the whole rocks (Holtzapffel, 1983).

From the 26 clay-size fractions <2 μm, two or three subfractions were separated by ultracentrifugation and studied by XRD and TEM. Depending on the amount of powder available, these subfractions were then analyzed for bulk chemistry, rare-earth element (REE) content, and Sr-, O-, and H-isotope compositions. The chemical composition of some individual flakes and laths were also determined by STEM. Details of the analytical procedures were described by Holtzapffel (1983).

RESULTS AND DISCUSSION

Mineralogy and morphology

The XRD data indicate that smectite was the dominant mineral phase in all samples, but that it was commonly mixed with other clays (illite, chlorite, kaolinite, mixed-layer illite/smectite, sepiolite and/or palygorskite), calcite, quartz, feldspars, goethite, opal, and/or clinoptilolite (Table 1). Measured using Biscaye's (1965) procedure, the crystallinity of the smectite indicated that the smaller particles were better crystallized than the larger particles. The position of the 060 smectite peak on the XRD patterns did not vary with particle size, suggesting that the overall chemical composition of the smectite population was fairly homogeneous. The position of the 060 peak was also systematically indicative of a dioctahedral type.

TEM observation revealed three types of smectite morphologies: (1) flake-like particles having diffuse and

https://doi.org/10.1346/CCMN.1990.0380105 Published online by Cambridge University Press

https://doi.org/10.1346/CCMN.1990.0380105 Published online by Cambridge University Press

Table 1. X-ray powder diffraction analyses of the marine sediments.

Samples	Location	Stratigraphic age	Whole-rock mineralogy						Clay-fraction mineralogy (%)									
			C	Q	F	Cp	Op	G	Chl	Ill	Ml	Sm	K	Fc	Q	F	Cp	Op
1 AG	Wissant	Middle Albian	+	+					Tr	20	Tr	70	10		+	++		
1 ET	Mol 359.5 m	Ypresian		+++	++				Tr	10	Tr	90	Tr		Tr	+	Tr	Tr
4 ET	Mol 562.2 m	Heersian	+++	+	Tr	+	Tr			Tr	Tr	100			Tr	Tr	+	
6 ET	Kallo 411 m	Landenian	+	+++	Tr	Tr	++			15	10	75			Tr	Tr		+++
8 ET	Cap d'Ailly	Thanetian	+	+++				+				100			++			
10 ET	Mt de la Chapelle	Thanetian		+++	+					15	Tr	85			+	Tr		
11 ET	Mt de la Chapelle	Thanetian		++	Tr	+				5	Tr	95	Tr					
12 ET	Boiry Notre Dame	Thanetian		++	++	Tr	Tr			10	Tr	90			+	Tr	Tr	
1 EM	DSDP 386.33.3, 100	Lower Eocene	+	+	Tr	+	Tr			10	Tr	90	Tr		+	Tr	++	Tr
18 EM	119.30.6, 100	Upper Palaeocene	+++	Tr	+	Tr	Tr		Tr	15		85	Tr	Tr	Tr	Tr	Tr	Tr
20 EM	119.31.3, 50	Upper Palaeocene	+++	+			+		Tr	10		90	Tr	Tr	+	+	Tr	+
22 EM	398.33.2, 50	Lower Eocene	+++	+	+	Tr	Tr		Tr	25	Tr	45	10	20	+	+		++
25 EM	398.34.2, 100	Lower Eocene	+++	Tr			Tr		Tr	10	Tr	40	5	45	+++	Tr	Tr	
29 EM	398.35.6, 70	Upper Palaeocene	++	+	++	Tr	Tr		Tr	20	Tr	70	5	5				
1 BS	105.14.1, 120	Aptian-Albian	Tr	++	++	+++	Tr		Tr	5	Tr	95		Tr		Tr		Tr
3 BS	105.15.3, 100	Aptian-Albian	Tr	+		++	Tr		Tr	10	Tr	90			Tr	Tr	Tr	Tr
6 BS	105.15.6, 110	Aptian-Albian	+	+		+++			Tr	10	Tr	90		Tr	Tr	Tr	+	Tr
16 BS	400.65.1, 100	Albian	+++	+	Tr		+		Tr	10	Tr	90			Tr	Tr	+	Tr
18 BS	400.69.1, 50	Upper Aptian	+++	+	Tr		Tr		Tr	5	Tr	95			Tr		Tr	
20 BS	402.15.2, 100	Albian	+	++		+	+			10	80	10			Tr		++	++

C = calcite; Q = quartz; F = feldspars; Cp = clinoptilolite; Op = opal; G = goethite; Chl = chlorite; Ill = illite; ML = mixed-layer illite/smectite; Sm = smectite; K = kaolinite; FC = fiber-type clays; Tr = traces; + = common; ++ = abundant; +++ = very abundant.

The locations refer to Figure 1. The DSDP samples are outlined as usual for this material.

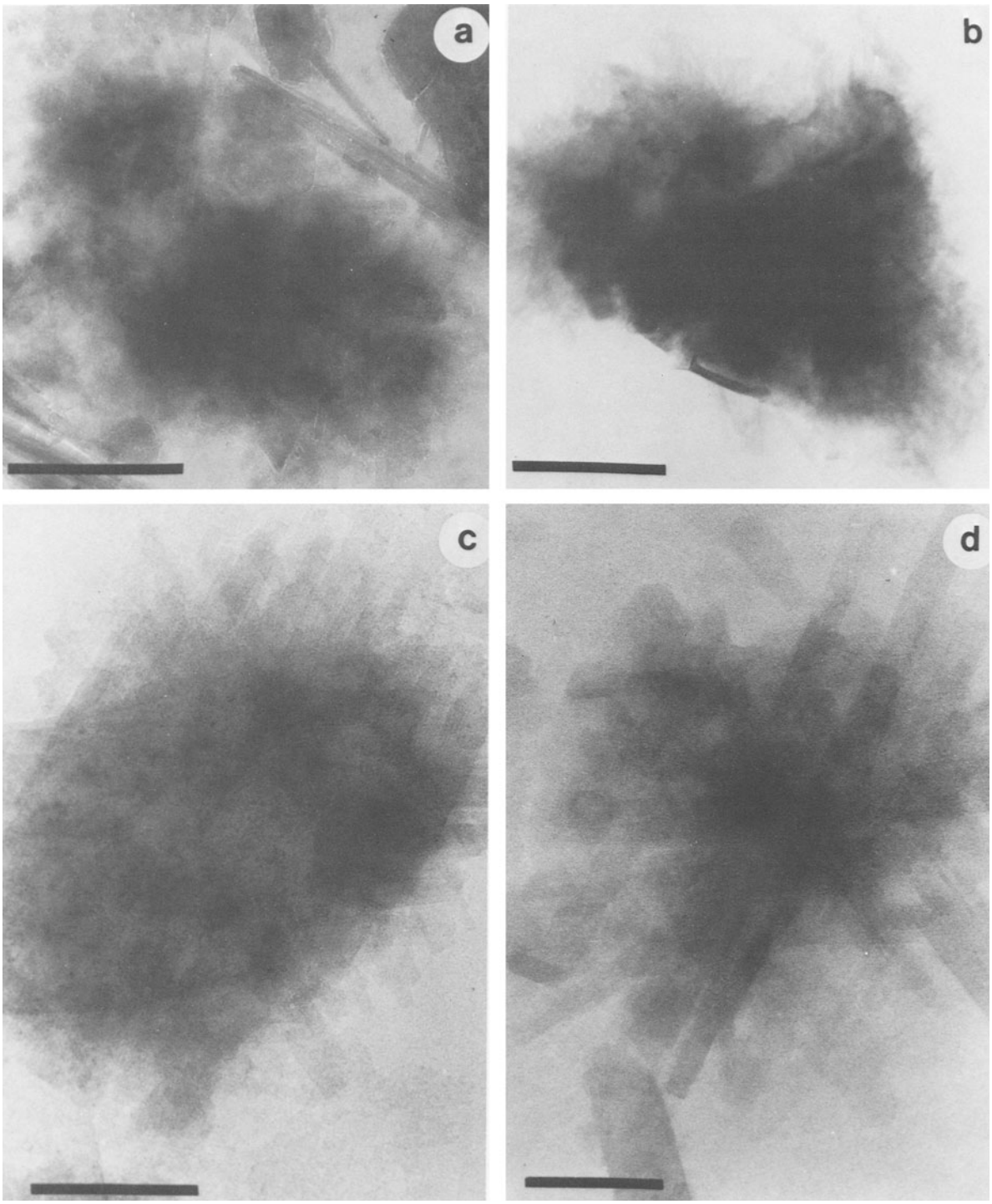

Figure 2. Transmission electron micrographs of different smectite morphologies: (a) flake-like particle and a few laths of palygorskite, bar length = 0.5 μm; (b) flake-like particle surrounded by fine fibers, bar length = 1 μm; (c) mixed assemblage of particle: flake-like particle surrounded by large laths, bar length = 0.5 μm; (d) lath-like particles oriented at 60° or 120° to one another, bar length = 0.2 μm.

https://doi.org/10.1346/CCMN.1990.0380105 Published online by Cambridge University Press

irregular borders more or less rolled-up, (2) lath-like, elongate, and euhedral particles oriented to each other at 60° or 120°, and (3) an intermediate type of morphology in which flake-like particles were surrounded by lath-like particles (Figure 2). The flake-like smectite has been described in other sedimentary sequences from the Atlantic Ocean (Chamley *et al.*, 1983) and was considered to be a detrital variety having originated from continental soils or rocks. The laths and the mixed shapes have been described in only a few studies (Hoffert, 1980; Louail, 1981; Jeans *et al.*, 1982; Clauer *et al.*, 1984). The possibility that mixture of flakes and laths could have resulted from an aggregation of laths stuck onto the flakes required special care to be taken in the preparation of the fractions for TEM observations. A vigorous ultrasonic dispersion was applied to those samples to avoid artifacts due to sample preparation. Despite that treatment, mixtures of laths and flakes were common, suggesting that they do indeed represent a transitional stage between the two other types. The flakes and the mixed assemblages were dominant in the coarser subfractions, whereas the laths were systematically enriched in the finer subfractions.

The interpretation of compositional data of multicomponent mixtures of variable proportions is difficult. The amount of each type of smectite was therefore estimated by mineral point counts in size fractions using TEM micrographs. This technique provides relative amounts of mineral surfaces not volumes, because the particles were settled in water drops for TEM observation. We therefore assumed a similar thickness for all particles. To increase the accuracy of the method, the counts were made by the same investigator systematically on two different particle-size fractions of the same sample. The finer subfractions always contained more laths (Table 2); the data being reproducible at ±5% (Holtzapffel and Chamley, 1986).

Table 2. Particle counts from transmission electron micrographs.

Samples		Flakes (%)	Mixed (%)	Laths (%)
1 AG	<0.5 μm	40	15	45
	<1 μm	45	20	35
4 ET	<0.5 μm	55	20	25
	<1 μm	75	15	10
11 ET	<0.5 μm	65	15	20
12 ET	<0.5 μm	50	20	30
	<1 μm	70	15	15
6 EM	<0.5 μm	35	10	55
9 EM	<0.4 μm	45	15	40
	<2 μm	55	25	20
1 BS	<0.5 μm	15	5	80
	0.5–2 μm	25	55	20
	<2 μm	25	35	40
3 BS	<0.5 μm	25	15	60
	0.5–2 μm	30	45	25
	<2 μm	30	25	45
6 BS	<0.5 μm	20	10	70
	0.5–2 μm	30	45	25
	<2 μm	25	30	45
16 BS	<0.5 μm	20	15	65
18 BS	<0.4 μm	30	15	55
	0.4–0.8 μm	60	15	25
	0.8–2 μm	85	15	0
20 BS	<0.5 μm	60	15	25
	<1.5 μm	65	25	10

Several size-fractions were observed for each sample.
Flakes, mixed, and laths stand for flake-like, mixed assemblages, and lath-like morphologies, respectively.

Major and rare-earth element compositions

The chemical data, obtained either by atomic absorption or by electron microprobe analyses of powders, were similar for different subfractions of the same sample (Table 3). Differences in samples 14BS, 16BS, 18BS, 6EM, 9EM, and 6ET can be attributed to contaminants, such as opal, calcite, goethite, or illite, which increased the contents of Si, Ca, Fe and K, respectively. The chemical data of the fractions containing about the same amount of smectite suggested that (1) the flake-type smectite is an Al-Fe variety, and (2) the laths in the finer fractions were chemically similar to the flakes, because their occurrence did not signifcantly change the chemistry of these fractions.

The REE were analyzed in several size fractions because these elements are thought to be accurate tracers for the origin of supergene minerals. The total amounts of the REE were relatively constant (Table 4). The distribution patterns were similar to those of the common shales (Figure 3; Haskin *et al.*, 1968; Piper, 1974) and to those of other samples from DSDP hole 398 (leg 47B; Courtois and Chamley, 1978). The patterns of the Albian- and Aptian-age samples were, for example, similar to Valanginian clay fractions of DSDP hole 105 for content and distribution (Chamley and Bonnot-Courtois, 1981). The strong negative Ce anomaly, which is typical of seawater-derived material (Goldberg *et al.*, 1963; Hogdhal *et al.*, 1968), was not detected even in the finest fractions enriched in laths. In sample 4ET a slight Ce anomaly was noted, probably due to the presence of clinoptilolite, which usually results from an alteration of volcanic material by seawater (Figure 3). The absence of a Ce anomaly contrasts sharply with the patterns of minerals newly formed in marine environments, which also contain more REE (Spirn, 1965; Bernat, 1973; Piper, 1974; Courtois and Hoffert, 1977). The present results suggest that the laths derived from preexisting detrital flakes by an isochemical dissolution-crystallization mechanism, without external input. The crystallization process of the laths here was different from that of the laths from southern Pacific deep-sea red clays, which have pronounced negative Ce anomalies, suggesting an influence of seawater (Bonnot-Courtois, 1981).

Chemical determinations were obtained by STEM

https://doi.org/10.1346/CCMN.1990.0380105 Published online by Cambridge University Press

https://doi.org/10.1346/CCMN.1990.0380105 Published online by Cambridge University Press

Table 3. Chemical analyses by atomic absorption and electron microprobe.

Samples	Location	Stratigraphic age	Atomic adsorption data								Electron microprobe data						
			SiO_2	Al_2O_3	Fe_2O_3	CaO	MgO	Na_2O	K_2O	TiO_2	SiO_2	Al_2O_3	Fe_2O_3	CaO	MgO	K_2O	TiO_2
1 AG WR	Wissant	Middle Albian	57.10	12.36	7.31	6.08	1.72	0.73	3.22	0.25							
<2 μm			50.05	21.30	7.57	1.09	2.61	0.15	3.63	0.29							
1 ET WR	Mol 359.5 m	Ypresian	67.75	12.10	5.63	1.22	1.76	1.05	2.26	0.44							
<2 μm			55.60	16.95	8.01	0.65	2.91	0.16	2.42	0.37							
4 ET 0.4–0.6 μm	Mol 562.2 m	Heersian									66.4	18.5	7.82	1.53	1.80	1.87	1.45
0.6–2 μm											67.8	16.2	8.13	1.27	1.45	2.05	1.41
6 ET <0.4 μm	Kallo 411 m	Landenian									77.5	10.8	8.24	0.20	1.02	1.98	0.22
0.4–1 μm											88.0	5.9	3.45	0.18	0.21	1.48	0.18
8 ET WR	Cap d'Ailly	Thanetian	75.65	6.68	3.50	4.31	0.63	0.04	0.04	0.20							
<2 μm			53.85	17.89	10.20	2.86	1.75	0.03	0.08	0.52							
10 ET WR	Mt de la Chapelle	Thanetian	72.75	11.05	3.89	0.82	1.75	0.19	2.21	0.31							
<2 μm			55.25	18.10	6.67	0.62	2.91	0.14	2.57	0.42							
11 ET WR	Mt de la Chapelle	Thanetian	61.80	13.80	8.36	1.57	1.21	0.21	1.46	0.65							
<2 μm			60.75	19.44	11.06	1.50	1.89	0.15	1.82	0.90							
12 ET WR	Boiry-Notre Dame	Thanetian	60.40	15.82	6.21	2.50	2.48	0.18	2.65	0.42							
<2 μm			53.95	17.01	7.12	1.19	2.70	0.12	2.73	0.36							
6 EM <2 μm	DSDP 386.34.5, 85	Upper Palaeocene	54.50	16.30	4.91	6.66	3.01	0.48	2.07	0.22							
8 EM <2 μm	387.22.3, 100	Lower Eocene	77.90	9.30	2.69	0.92	1.61	0.48	1.28	0.16							
9 EM <2 μm	387.23.5, 50	Lower Eocene	54.40	17.10	8.71	1.04	3.32	0.76	2.97	0.32							
11 EM <2 μm	387.23.5, 50	Upper Palaeocene	53.90	18.60	7.86	1.46	3.02	1.11	2.92	0.33							
14 EM <2 μm	119.29.3, 100	Upper Palaeocene	58.50	17.05	7.85	1.51	2.95	0.28	2.45	0.22							
22 EM <0.4 μm	398.33.2, 50	Lower Eocene									60.5	22.3	6.80	0.51	5.37	3.41	—
0.4–2 μm											58.1	25.3	6.06	0.66	2.85	5.48	1.50
25 EM <0.4 μm	398.34.2, 100	Lower Eocene									63.7	17.1	6.74	1.05	8.97	1.97	0.50
0.4–2 μm											61.9	22.4	5.64	0.72	3.08	4.81	1.12
29 EM <2 μm	398.35.6, 70	Upper Palaeocene	51.90	19.70	7.22	2.12	3.62	0.46	3.40	0.26							
1 BS <0.2 μm	105.14.1, 120	Aptian-Albian									64.2	20.0	8.66	0.74	3.57	2.34	0.51
0.2–0.4 μm											64.2	20.2	8.11	0.97	3.36	2.60	0.53
0.4–2 μm											66.0	19.5	6.53	0.80	2.66	3.30	1.21
3 BS <0.4 μm	105.15.3, 100	Aptian-Albian									62.8	20.9	9.01	0.59	3.40	2.80	0.62
0.4–2 μm											64.1	20.6	7.45	0.63	3.20	3.20	0.78
6 BS <2 μm	105.15.6, 110	Aptian-Albian	51.80	17.70	8.70	0.50	3.16	0.37	1.89	0.22							
14 BS <0.2 μm											58.7	16.6	13.56	0.68	5.11	4.95	0.35
0.2–2 μm											77.1	9.4	7.30	0.38	2.39	2.91	0.51
16 BS <2 μm	400.65.1, 50	Albian	42.30	15.80	5.02	11.46	2.04	0.49	2.57	0.26							
18 BS <0.4 μm	400.69.1, 50	Upper Aptian									62.3	16.9	12.58	3.25	2.87	1.80	0.33
0.4–0.8 μm											59.0	16.6	10.58	8.84	2.33	2.10	0.38
0.8–2 μm											57.0	14.6	9.59	14.67	1.56	2.20	0.39
20 BS <2 μm	402.15.2, 100	Albian	54.90	20.35	4.26	0.91	1.48	0.25	1.83	0.33							

For details of locations, see Table 1; WR = whole rocks; all amounts in %.

Table 4. Rare-earth element determinations by neutron activation analysis (μg/g).

Sample	La	Ce	Nd	Sm	Eu	Tb	Yb	Lu	Total	La/Yb
1 AG <0.2 μm	19.0	36.5	16.5	3.00	0.70	0.50	1.40	0.25	78	13.6
0.2–0.4 μm	15.2	31.3	13.5	2.70	0.50	0.37	1.00	0.20	65	15.2
4 AG <0.1 μm	30.0	60.0	27.0	5.10	0.80	0.60	1.80	0.30	125	16.6
0.1–2 μm	22.5	42.0	19.0	3.60	0.60	0.40	1.40	0.25	90	16.1
1 ET <0.4 μm	21.5	45.4	21.0	4.60	0.85	0.60	1.70	0.28	96	12.6
0.4–0.6 μm	23.9	49.5	25.0	4.80	0.95	0.70	2.10	0.37	107	11.4
0.6–2 μm	34.0	70.0	32.0	6.50	1.30	1.00	2.90	0.50	148	11.7
4 ET <0.4 μm	12.8	16.1	9.5	2.20	0.45	0.37	1.10	0.20	43	11.6
<2 μm	17.5	25.0	12.0	2.50	0.60	0.42	1.20	0.22	59	14.6
6 ET <0.4 μm	16.9	32.0	15.0	3.10	0.50	0.30	0.65	0.10	68	25.4
8 ET 0.2–0.4 μm	12.0	27.0	10.0	2.20	0.45	0.35	0.85	0.15	53	14.1
10 ET <0.4 μm	30.0	56.0	30.0	6.50	1.00	0.75	2.20	0.38	127	13.6
0.4–0.6 μm	37.0	68.5	30.0	6.50	1.15	0.80	2.40	0.42	147	15.4
0.6–2 μm	44.5	73.3	35.0	7.00	1.25	0.85	2.55	0.45	165	17.4
11 ET <0.4 μm	29.7	51.5	27.0	6.20	1.40	1.00	2.50	0.42	120	11.9
0.4–0.8 μm	32.6	59.0	30.0	6.80	1.60	1.20	2.30	0.40	134	14.2
12 ET <0.4 μm	45.5	82.5	38.0	7.80	1.80	1.30	2.65	0.43	180	17.1
0.4–0.8 μm	46.0	80.0	36.5	7.50	1.70	1.30	2.30	0.42	176	20.0
0.8–2 μm	52.0	92.0	37.5	7.80	1.90	1.50	2.90	0.50	196	17.9
6 EM <0.4 μm	15.5	30.4	13.5	2.35	0.45	0.31	0.90	0.15	63	17.2
0.4–0.8 μm	19.0	37.5	15.0	2.90	0.50	0.38	1.10	0.20	76	17.3
0.8–2 μm	21.3	43.6	19.0	3.50	0.68	0.50	1.40	0.25	90	15.2
1 BS <0.2 μm	18.5	38.0	15.2	2.63	0.56	0.40	1.08	0.18	76	17.1
3 BS <0.4 μm	30.0	58.0	25.0	4.35	0.95	0.75	2.10	0.34	121	14.3
14 BS <0.2 μm	73.0	123.0	68.0	15.0	3.00	2.20	5.50	0.80	290	13.3
0.2–2 μm	69.0	110.0	56.0	10.5	1.90	1.40	3.70	0.60	253	18.6
18 BS <0.4 μm	22.2	48.5	22.0	4.55	0.85	0.60	1.80	0.30	101	12.3
0.4–0.8 μm	19.0	37.5	15.0	2.90	0.50	0.38	1.10	0.20	76	17.3
0.8–2 μm	36.5	67.0	30.0	6.00	1.30	0.80	2.30	0.40	144	15.8

by secondary X-ray spectrometry using a 20–30-Å beam. This procedure allowed measurements to be made on individual laths and flakes. The flakes ranged slightly in chemical composition, but the scatter was not size-dependent (Steinberg *et al.*, 1984, 1987). The laths, on the other hand, had higher Si/Fe ratios and gave more uniform data, suggesting an homogenization process during dissolution-crystallization. This slight change in the chemical composition suggests that the crystallization of laths on detrital beidellite and illite did not occur in a completely closed system. The results are compatible with a migration of elements, such as Fe, over very short distances.

Strontium isotope compositions

The Rb-Sr isotope method was applied to size fractions of 12 clay samples using procedures similar to those outlined by Clauer (1976). Each size fraction was leached with 1 N HCl for 15 min at room temperature prior to isotope measurement. This treatment removed the Sr which had not already been removed by distilled water and which might have been present in easily exchangeable interlayer sites, on grain surfaces, or in soluble authigenic minerals, and left the Sr which was trapped in the mineral structures during crystallization or later alteration (Clauer, 1982; Clauer *et al.*, 1984). Three Rb-Sr determinations were made, if possible, for each size fraction: one on the untreated sample, one on the leachate, and one on the residue (Tables 5 and 6). The data points for each size fraction plotted along lines with different slopes on isochron diagrams (Figure 4). These lines were considered mixing lines and not isochrons, because the subfractions contained mixtures of minerals of different sources having different initial $^{87}Sr/^{86}Sr$ ratios.

Leaching experiments have been used for a long time in attempts to date sedimentary rocks and minerals by isotope methods, especially for removing the Sr-rich carbonate fractions (Bofinger *et al.*, 1968). General agreement has, however, never been reached on the type of reagent to be used to avoid preferential extraction of radiogenic ^{87}Sr from the clay structure. We used 1 N HCl, because Kralik (1984) recently demonstrated that leaching a sedimentary illite with 1 N HCl did not affect the radiogenic ^{87}Sr more than a treatment with a cation-exchange resin or than a leaching with 5% NH_4-EDTA, and because Clauer *et al.* (1986) obtained similar results by leaching a diagenetic illite with 1 N HCl. Many published data are unnecessarily scattered, suggesting experimental artifacts during the procedure leading to erroneous interpretations (Dasch, 1969; Morton and Long, 1980; Macedo de Freitas, 1982). A

https://doi.org/10.1346/CCMN.1990.0380105 Published online by Cambridge University Press

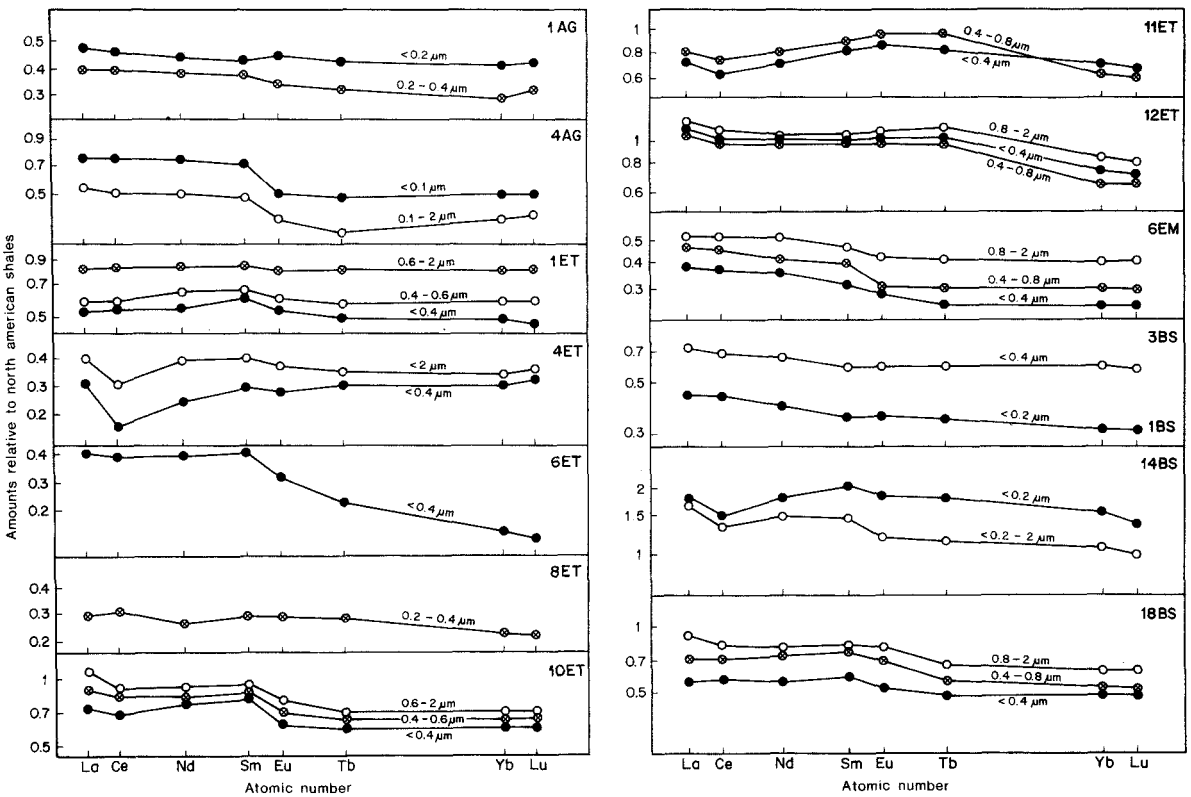

Figure 3. Distribution patterns of rare-earth elements of size sub-fractions of different samples, normalized to North American shales.

careful control of the technique is therefore needed to analyze the untreated sample, the leachate, and the residue. The data must plot on a straight line on an isochron diagram, and the amounts of Rb and Sr measured in the untreated sample must equal the sum of those in the leachate and residue. This control was applied to several samples in the present investigation (Table 5); the differences between measured and calculated amounts of Rb and Sr in the untreated samples and in the leachates and residues never exceeded 4.5%, except for sample 18 BS, in which the Sr differed by 15.7%.

As 1 N HCl leaching experiments do not preferentially remove radiogenic ^{87}Sr from clay mineral structures, the $^{87}Sr/^{86}Sr$ of the leachate was considered to be identical to that of the interstitial environment in contact with the particles, as shown in other studies on Recent clay material (Hoffert *et al.*, 1978; Clauer *et al.*, 1982; Clauer and Hoffert, 1985). If the clay particles reacted after deposition, they undoubtedly did it with this environment, and an analysis of the removable Sr may provide some important information about the nature of the reaction. If the leached Sr has the same $^{87}Sr/^{86}Sr$ ratio as seawater, (1) the detrital particles did not react with the aqueous environment, (2) mineral precipitation occurred directly from fluids without dissolution of the detrital material, or (3) reorganization of detrital material occurred in an open system with a large water/rock ratio. The Sr of the interstitial environment may also have an $^{87}Sr/^{86}Sr$ ratio different from that of the marine environment. Not considering the decay of ^{87}Rb to ^{87}Sr in the water, this ratio might be higher than the seawater value, if detrital material alters to a new mineral phase in a closed system. In this case, the detrital components will supply an "excess" of ^{87}Sr to the waters. If material of volcanic origin alters into a new mineral phase, the $^{87}Sr/^{86}Sr$ ratio of the aqueous environment may decrease, if the system remains closed. Consequently, the more authigenic material in a closed system, the greater should be the difference between the $^{87}Sr/^{86}Sr$ ratio of the interstitial waters and that of the seawater.

Most of the Sr isotope data referred to here support the hypothesis of a dissolution-crystallization process in a closed system in which the $^{87}Sr/^{86}Sr$ ratios of the leachates were greater than that of the corresponding seawater (Tables 5 and 6). The $^{87}Sr/^{86}Sr$ values of seawater varied in Albian and Aptian times from 0.70755 to 0.70722 (Faure, 1982), and those of seawater in Palaeocene time averaged 0.70777 ± 10 (Hess *et al.*,

https://doi.org/10.1346/CCMN.1990.0380105 Published online by Cambridge University Press

Table 5. Control of the Rb-Sr leaching procedure.

Samples[1]		% of untreated size-fraction	Rb measured (μg/g)	Rb calculated (μg/g)	Sr measured (μg/g)	Sr calculated (μg/g)	App. ages (Ma)	Initial $^{87}Sr/^{86}Sr$
4 ET <2 μm	U		81.8		91.4		161 ± 9	0.70767 ± 27
	L	3.23	192	6.2	1021	33.0		
	R	96.77	78.6	76.1	60.6	58.6		
	L + R			82.3		91.6		
8 ET 0.2–0.4 μm	U		1.90		37.5		130 ± 31	0.70788 ± 17
	L	0.55	64.9	0.36	5353	29.4		
	R	99.45	1.55	1.54	6.6	6.5		
	L + R			1.90		35.9		
11 ET <0.4 μm	U		111.5		73.5		231 ± 10	0.70651 ± 32
	L	1.87	289	5.4	943	17.6		
	R	98.13	111.6	109.5	59.9	58.8		
	L + R			114.9		76.4		
12 ET <0.4 μm	U		140.6		73.5		170 ± 7	0.70910 ± 25
	L	0.60	780	4.7	3709	22.2		
	R	99.40	138.2	137.4	53.7	53.4		
	L + R			142.1		75.6		
6 EM 0.8–2 μm	U		113.4		401		260 ± 13	0.70771 ± 20
	L	15.70	36.7	5.8	1755	275.5		
	R	84.30	129.3	109.0	132.3	111.5		
	L + R			114.8		387.0		
18 BS 0.8–2 μm	U		99.5		211		439 ± 8	0.70768 ± 11
	L	17.74	25.1	4.45	935	165.9		
	R	82.26	123.5	101.6	102.5	84.31		
	L + R			106.0		250.2		

[1] U = untreated size-fraction, L = leachate, R = residue, L + R = calculated sum of leachate + residue.
Initial $^{87}Sr/^{86}Sr$ ratios with errors in 10^{-5} at 2σ level.

1986). The contribution of ^{87}Sr from the decay of ^{87}Rb must be deduced from measured $^{87}Sr/^{86}Sr$ ratios for a more precise evaluation of the interstitial $^{87}Sr/^{86}Sr$, and this can be done by direct use of the intercepts of the mixing lines of the untreated subfractions, leachates, and residues (Figure 4). These lines represent mixtures of Rb and Sr trapped in the mineral structures and Rb and Sr removed from the clay particles by gentle leaching. Inasmuch as more Rb was removed by leaching than is present in interstitial waters, a correction for this excess was made by assuming that the value of the intercepts was the $^{87}Sr/^{86}Sr$ of the exchangeable Sr. This ratio increased as the amount of authigenic laths increased in the subfractions, i.e., as the size of the subfractions decreased (Figure 4). Sample 8 ET was analyzed to test *a contrario* this hypothesis because it contained no laths (Table 5 and 6). If the hypothesis is correct, the intercepts of all subfractions should be identical to that of the corresponding $^{87}Sr/^{86}Sr$ seawater ratio. The data for the smallest subfraction (<0.2 μm) gave a mixing line having an intercept at 0.70771 ± 17 ($2\sigma \times 10^{-5}$), that of the line for the intermediate subfraction (0.2–0.4 μm) averaged 0.70788 ± 18, and the intercept of the line for the coarsest subfraction (0.4–2 μm) gave 0.70788 ± 19, whereas the seawater value is 0.70777 ± 10.

Direct isotopic dating of the dissolution-crystallization process was not possible because all clay-size fractions were mixtures of detrital and authigenic particles. Clay minerals formed in continental soil profiles have widely scattered $^{87}Sr/^{86}Sr$ ratios (Clauer, 1979) and consequently a range of high Rb-Sr apparent ages. Furthermore, they interact with migrating waters in the soils (Thellier and Clauer, 1989) and thereby trap Sr. This reduces the Rb/Sr ratios and increases even more the Rb-Sr apparent ages. Rb-Sr apparent ages of any size fraction containing detrital clay particles are, therefore, meaningless in a rational time sense, because they integrate values of material of different origins with different Rb-Sr systematics. These apparent ages can, however, be related to the amounts of laths present in the size fractions by mass-balance calculations. Plotted against the lath contents of the different size fractions of the same sample, they allow extrapolations to pure authigenic end-members consisting of 100% laths, which should roughly approximate the formation time of these laths (Figure 5). The data systematically gave values of about 100 Ma and 60 Ma for the Cretaceous and the Palaeocene samples, respectively, which are close to the stratigraphic ages of the sequences. Consequently, the smectite was probably altered soon after deposition.

https://doi.org/10.1346/CCMN.1990.0380105 Published online by Cambridge University Press

Table 6. Rb-Sr isotope data.

Samples			Rb (μg/g)	Sr (μg/g)	$^{87}Rb/^{86}Sr$	$^{87}Sr/^{86}Sr$[1]	App. ages (Ma)	Initial $^{87}Sr/^{86}Sr$[2]
1 AG	<0.2 μm	L	242	1730	0.405	0.71047 ± 7	159 ± 6	0.70955 ± 20
		R	184.9	44.30	12.09	0.73695 ± 16		
	0.2–0.4 μm	L	199.9	896	0.647	0.71091 ± 14	190 ± 5	0.70917 ± 20
		R	183.5	43.30	12.28	0.74216 ± 10		
	0.4–2 μm	L	336	1098	0.887	0.71049 ± 17	218 ± 8	0.70774 ± 29
		R	184.3	64.80	8.246	0.73328 ± 13		
6 ET	<0.4 μm	L	143.8	1427	0.292	0.70988 ± 8	108 ± 5	0.70943 ± 18
		R	76.90	27.80	8.010	0.72172 ± 8		
	0.4–1 μm	L	116.5	350	0.964	0.70903 ± 14	235 ± 14	0.70581 ± 42
		R	38.90	27.60	4.092	0.71947 ± 12		
8 ET	<0.2 μm	L	6.55	5.81	0.033	0.70781 ± 9	221 ± 26	0.70771 ± 17
		R	1.91	5.34	1.048	0.71100 ± 10		
	0.4–2 μm	L	5.88	302	0.056	0.70806 ± 8	236 ± 114	0.70788 ± 19
		R	3.16	20.04	0.457	0.70971 ± 8		
11 ET	0.8–2 μm	L	173.3	626	0.803	0.70973 ± 15	286 ± 14	0.70647 ± 38
		R	121.9	74.50	4.774	0.72576 ± 12		
12 ET	0.4–0.8 μm	L	287	1139	0.730	0.71099 ± 10	202 ± 7	0.70889 ± 27
		R	168.8	51.50	9.501	0.73620 ± 18		
	0.8–2 μm	L	125.4	563	0.646	0.71037 ± 8	234 ± 9	0.70822 ± 28
		R	170.6	67.60	7.313	0.73254 ± 14		
6 EM	<0.4 μm	L	194.7	2588	0.218	0.70997 ± 7	156 ± 6	0.70838 ± 22
		R	55.50	15.47	10.39	0.73151 ± 5		
	0.4–0.8 μm	L	126.0	2210	0.165	0.70821 ± 9	229 ± 7	0.70822 ± 28
		R	134.9	52.70	7.420	0.73189 ± 7		
17 EM	<0.4 μm	L	349	2383	0.424	0.71021 ± 5	141 ± 4	0.70936 ± 19
		R	106.9	26.20	11.85	0.73316 ± 11		
	0.4–0.8 μm	L	619	2355	0.592	0.71016 ± 8	201 ± 8	0.70846 ± 26
		R	116.7	49.90	6.773	0.72786 ± 8		
	0.8–2 μm	L	215	1292	0.483	0.71030 ± 5	205 ± 11	0.70889 ± 25
		R	119.2	79.60	4.339	0.72153 ± 9		
22 EM	<0.4 μm	U	257	133.9	5.599	0.73152 ± 8		
		R	174.1	56.70	8.896	0.73398 ± 7		
	0.4–2 μm	L	800	8678	0.267	0.70880 ± 12	299 ± 10	0.70766 ± 21
		R	256	110.30	6.728	0.73628 ± 8		
3 BS	<0.4 μm	L	301	1371	0.636	0.71148 ± 6	167 ± 8	0.70997 ± 25
		R	132.4	71.20	5.392	0.72280 ± 10		
	0.4–2 μm	L	262	1071	0.725	0.71127 ± 5	219 ± 10	0.70901 ± 30
		R	154.7	779	5.758	0.72695 ± 7		
14 BS	<0.2 μm	L	61.30	810	0.219	0.70854 ± 11	153 ± 4	0.70806 ± 16
		R	165.6	21.20	22.62	0.75722 ± 11		
	0.2–2 μm	L	83.10	822	0.293	0.70837 ± 11	251 ± 9	0.70732 ± 31
		R	99.90	52.50	5.521	0.72703 ± 11		
18 BS	<0.4 μm	L	69.40	2540	0.079	0.70861± 10	154 ± 7	0.70844 ± 16
		R	95.90	48.80	5.693	0.72087 ± 13		
	0.4–0.8 μm	L	27.70	1294	0.062	0.70847 ± 9	193 ± 7	0.70830 ± 16
		R	112.50	51.40	6.350	0.72572 ± 10		

[1] Errors in 10^{-5} at $2\sigma/\sqrt{N}$ level.
[2] Initial $^{87}Sr/^{86}Sr$ ratios with errors in 10^{-5} at 2σ level.
U, L, and R stand for untreated, leachate, and residue, respectively.

Sample 4T contains clinoptilolite in addition to the different morphological types of smectite. This obviously authigenic zeolite apparently formed in the presence of a larger amount of sea water than the smectite, as evidenced by the slight negative Ce anomaly (Figure 3). These two minerals do not appear to have paragenetic relation because the crystallization of the clay mineral in a closed system did surely not take place at the same time as the precipitation of the zeolite in a more open system. The overall isotopic data of the mixture are, however, similar to those of the other samples, but the dating technique failed because of an obvious underestimation of the amount of the authigenic material, due to the fact that the clinoptilolite particles were not counted (Table 2).

Stable isotope compositions

Hydrogen and oxygen isotope compositions and H_2O+ contents were determined on two or three size-fractions of seven clay samples. The data are presented in Table 7 in the usual δ-notation relative to the SMOW standard. The $\delta^{18}O$ value of the NBS-28 quartz standard is 9.6‰, and the δD value of the NBS-30 biotite standard is −64.5‰ in the Menlo Park laboratory.

https://doi.org/10.1346/CCMN.1990.0380105 Published online by Cambridge University Press

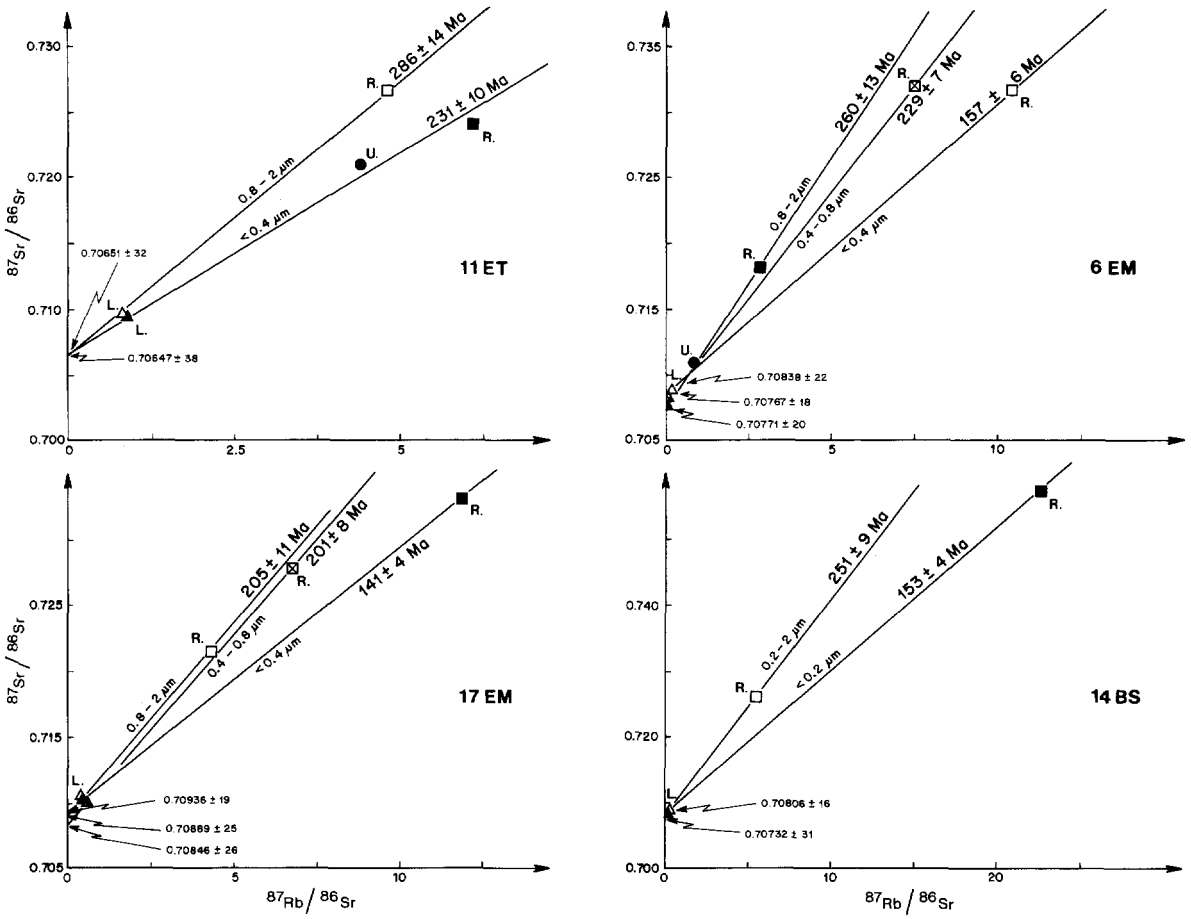

Figure 4. Isochron diagrams of untreated size subfractions, their leachates (L), and residues (R) after 1 N HCl leaching of four smectite-rich clay fractions.

The δD values of authigenic clay minerals of marine sediments are typically about −80 to −60‰ (Savin and Epstein, 1970b) and may depend on the chemical composition of the mineral. High Fe contents, for example, commonly correlate with low δD values (Suzuoki and Epstein, 1976), but this was not observed in the present samples. In fact, the sample containing the most Fe (18 BS) had the highest δD value. More importantly, such δD values (as well as water contents of 4–5%) are similar to those of many detrital clays and, as such, are not useful in distinguishing authigenic from detrital clays. The amount of hydrogen in clays, however, is relatively small, and, thus, detrital clays having unusually large or small δD values may be sensitive indicators of external additions or of exchange with external fluids during diagenesis.

Sample suites 1 ET, 12 ET, and 3 BS are noteworthy as they had particularly low and similar δD values of about −107‰. The former two suites represent the youngest samples analyzed. Collected on land, they could have undergone minor hydrogen isotope exchange with isotopically light ground waters, but based on stable isotope data, such an exchange process after diagenesis is highly unlikely (e.g., O'Neil, 1987). Sample 3BS, which has similar δD values, was collected from the sea and is one of the older samples (Upper Albian) examined. Thus, the low δD values appear to reflect the conditions in which the detrital clays were formed. The retention of these unusually low δD values during growth of authigenic laths strongly suggests that the pore waters were not in rapid communication with the open sea during diagenesis of these sediments.

In contrast to the hydrogen isotope compositions, oxygen isotope analyses are useful in distinguishing authigenic from detrital clay components. From analyses of detrital sediments from deep-sea cores, Savin and Epstein (1970b) estimated that the average $\delta^{18}O$ value of detrital smectites in ocean sediments is 17 ± 2‰. From determination of the oxygen isotope composition of <0.1-µm-size smectite from bottom sediments and coexisting interstitial waters, Yeh and Eslinger (1986) concluded that land-derived smectite is stable in seawater for as long as 25 Ma. Authigenic marine smectite forms at lower temperatures than

https://doi.org/10.1346/CCMN.1990.0380105 Published online by Cambridge University Press

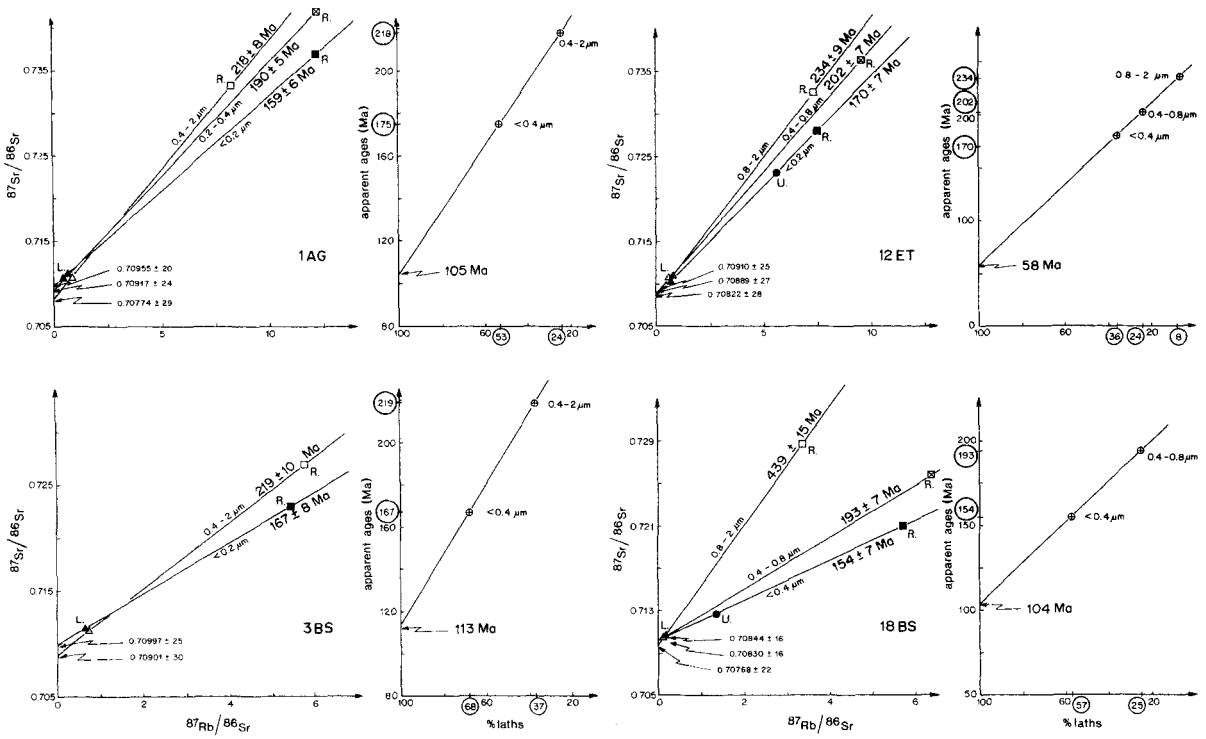

Figure 5. Isochron diagrams and age estimates of size subfractions of four smectite-rich clay fractions. For explanation of the symbols in the isochron diagrams, see legend of Figure 4.

smectite formed on land and in waters with a higher content of ^{18}O. Accordingly it has markedly higher $\delta^{18}O$ values of about 26–31‰ (Savin and Epstein, 1970a; Yeh and Savin, 1976). Oxygen isotope compositions, thus, can clearly discriminate between detrital and authigenic smectite found in ocean sediments. This is particularly important if no chemical or mineralogical differences can be utilized in making this distinction.

Table 7. Stable isotope data and the water content.

Samples		$^{18}O^1$	D^1	H_2O^2
1 AG	<0.2 μm	+18.1	−83	6.4
	0.2–0.8 μm	+17.4	−85	7.0
1 ET	<0.4 μm	+21.5	−107	5.3
	0.4–0.6 μm	+21.3	−107	5.3
	0.6–2 μm	+19.9	−102	5.0
12 ET	<0.4 μm	+21.5	−102	4.9
	0.4–0.8 μm	+20.0	−108	4.9
6 EM	<0.4 μm	+21.8	−89	5.2
	0.4–0.8 μm	+21.6	−96	6.5
	0.8–2 μm	+21.8	−79	4.0
17 EM	<0.4 μm	+23.6	−86	5.1
	0.8–2 μm	+23.0	−76	4.9
3 BS	<0.4 μm	+20.5	−107	5.6
	0.4–2 μm	+19.2	−108	5.0
18 BS	<0.4 μm	+21.6	−81	5.2
	0.4–0.8 μm	+22.5	−88	4.5
	0.8–2 μm	+21.5	—	—

[1] In ‰ relative to SMOW.
[2] In percent.

The most obvious aspect of the oxygen isotope data presented here is that almost all of the fine subfractions, which contained most of the newly crystallized minerals, had $\delta^{18}O$ values closer to those of normal detrital minerals than to those of authigenic clays. Sample 17 EM, which had a relatively high $\delta^{18}O$ value of 23.6‰ for the smallest subfraction, had a detrital component that was already high at 23.0 permil in the coarsest subfraction. In every sample the $\delta^{18}O$ values increased from the coarse to the fine subfraction, except for sample 6 EM, in which it remained the same, and sample 18 BS in which the highest value was measured for the intermediate subfraction. The maximum increases measured for $\delta^{18}O$ were at 1.4, 1.5, and 1.6‰, whereas the minimum increases were at 0.6 and 0.7‰. The question remains, what amount of increase in ^{18}O content should have occurred if the newly formed minerals, whose amount was estimated from the TEM photographs, grew in the presence of sea water? If $\delta^{18}O$ values of 18 and 28‰ are assumed for a typical detrital and authigenic smectite, respectively, a 50-50 mixture of these components should have a $\delta^{18}O$ value of 23‰. This value corresponds to an increase of 5‰ from a mainly detrital coarse subfraction to the finest subfraction, an increase much larger than observed for similar amounts of authigenic minerals in the samples examined here. Thus, if the detrital components were clearly richer in ^{18}O, either because they formed under

https://doi.org/10.1346/CCMN.1990.0380105 Published online by Cambridge University Press

the appropriate conditions during weathering on land or because the coarser fraction analyzed contained neoformed material, the expected increase in $\delta^{18}O$ should have been lower.

The lack of a significant increase in $\delta^{18}O$ for some fine subfractions containing >50% authigenic smectite is striking. The oxygen isotope compositions of the coarse and fine subfractions of samples 6 EM and 18 BS were identical, which again supports the conclusion that the diagenesis of these sediments took place under conditions of very low water/rock ratio, without significant input of external fluids. Yeh and Savin (1977) and Eslinger and Savin (1973) suggested that similar conditions prevailed during burial diagenesis and metamorphism in the Gulf Coast and Belt Series sediments. Thus, authigenic sedimentary clays should have high $\delta^{18}O$ values only if they form under conditions of high water/rock ratio, as in halmyrolysis reactions or direct precipitation in open sea conditions. In shales, on the other hand, detrital smectites probably recrystallize in limited amounts of pore water; this behavior might therefore be a general rule during shale diagenesis and low-grade metamorphism.

SUMMARY AND CONCLUSIONS

Detrital smectite from marine sediments, mainly shales, from the northern Atlantic, Belgium, and northern France underwent alteration that was detected by morphological observations (TEM), chemical analyses (major and rare-earth elements), and isotopic determinations (Sr, O, H). The chemical and isotopic compositions of detrital flake-like smectite particles and authigenic lath-like smectite particles were almost identical, probably because of a dissolution-crystallization process in a relatively closed environment. This environment had, however, to be permeable enough to allow short-distance mobility of cations, such as Fe, in the interstitial fluids.

The dissolution-crystallization process probably occurred soon after deposition. Further compaction does not appear to have had a noticeable effect on the clay particles, inasmuch as those collected from outcrops on land had the same characteristics as those recovered from the ocean. Inasmuch as the sediments examined were mainly shales of diverse age and type, the relatively closed-system recrystallization described here may be a common process operative during early and late diagenesis of shales.

ACKNOWLEDGMENTS

We sincerely thank H. Chamley (University of Lille) and M. Steinberg (University of Orsay) for their continuing interest in this study and for constructive discussions and S. M. Savin (Case Western University, Cleveland, Ohio) and an anonymous reviewer for their thoughtful and accurate comments. We are also indebted to B. Kiefel, D. Tisserant, R. A. Wendling, and R. Winkler of the Centre de Géochimie de la Surface (Strasbourg, France), and L. Adami of the U.S. Geological Survey (Menlo Park, California) for technical assistance. This study was supported by the Action Thématique sur Programme "Géologie et Géophysique des Océans."

REFERENCES

Arthur, M. A. (1979) North Atlantic Cretaceous black-shales: The record at site 398 and a brief comparison with other occurrences: in *Initial Reports of the Deep Sea Drilling Project, 47, Part 2,* J. C. Sibuet, W. B. F. Ryan, *et al.,* eds., U.S. Gov. Print. Office, Washington, D.C., 719–751.

Bernat, M. (1973) Les terres rares dans le milieu marin: Thèse Doc. Sciences, Univ. Paris VI, Paris, France, 1–25.

Biscaye, P. (1965) Mineralogy of Recent deep-sea clay in the Atlantic Ocean and adjacent seas and oceans: *Geol. Soc. Amer. Bull.* **76,** 803–832.

Bofinger, V. M., Compston, W., and Vernon, M. J. (1968) The application of acid leaching to the Rb-Sr dating of a Middle Ordovician shale: *Geochim. Cosmochim. Acta* **32,** 823–833.

Bonnot-Courtois, C. (1981) Géochimie des terres rares dans les principaux milieux de formation et de sédimentation des argiles: Thèse Doc. Sciences, Univ. Orsay, Orsay, France, 217 pp.

Chamley, H. (1979) North Atlantic clay sedimentation since the Late Jurassic: in *2nd Ewing Symposium,* Amer. Geophysical Union Publication, New York, 342–361.

Chamley, H. and Bonnot-Courtois, C. (1981) Argiles terrigènes et authigènes de l'Atlantique et du Pacifique NW (Leg II et 58 DSDP): Apport des terres rares: *Oceanol. Acta* **4,** 229–238.

Chamley, H. and Debrabant, P. (1982) L'Atlantique Nord à l'Albien: Influences américaines et africaines sur la sédimentation: *C.R. Acad. Sci., Paris* **294D,** 525–528.

Chamley, H., Debrabant, P., Candillier, A. M., and Foulon, J. (1983) Clay mineralogical and inorganic geochemical stratigraphy of Blake-Bahama Basin since the Callovian, site 534 Deep Sea Drilling Project leg 76: in *Initial Reports of the Deep Sea Drilling Project, 76,* R. E. Sheridan, R. M. Gradstein, *et al.,* eds., U.S. Gov. Print. Office, Washington, D.C., 437–542.

Clauer, N. (1976) Géochimie isotopique du strontium des milieux sédimentaires. Application à la géochronologie de la couverture du craton ouest-africain: *Mém. Sci. Géol., Strasbourg* **45,** 256 pp.

Clauer, N. (1979) Relationship between the isotopic composition of strontium in newly formed continental clay minerals and their source material: *Chem. Geol.* **27,** 115–124.

Clauer, N. (1982) Strontium isotopes of Tertiary phillipsites from the southern Pacific. Timing of the chemical evolution: *J. Sed. Petrol.* **52,** 1003–1009.

Clauer, N., Chaudhuri, S., and Massey, K. W. (1986) Relationship between clay minerals and environment by the Sr isotopic composition of their leachates: *Abstracts with Programs, Annual Meeting Geol. Soc. Amer., San Antonio, Texas,* 565–566.

Clauer, N., Giblin, P., and Lucas, J. (1984) Sr and Ar isotope studies of detrital smectites from the Atlantic Ocean (DSDP legs 43, 48, and 50): *Isot. Geosc.* **2,** 141–151.

Clauer, N. and Hoffert, M. (1985) Sr isotopic constraints for the sedimentation rate of deep sea red clays in the Southern Pacific Ocean: in *The Chronology of the Geological Record,* N. J. Snelling, ed., *Mem. Geol. Soc. London* **10,** 290–296.

Clauer, N., Hoffert, M., and Karpoff, A. M. (1982) The Rb-Sr isotope system as an index of origin and diagenetic evo-

https://doi.org/10.1346/CCMN.1990.0380105 Published online by Cambridge University Press

lution of southern Pacific red clays: *Geochim. Cosmochim. Acta* **46,** 2659–2664.

Cool, T. (1982) Sedimentological evidence concerning the paleooceanography of the Cretaceous western North Atlantic Ocean: *Paleogeogr. Paleoclim. Paleoecol.* **39,** 1–35.

Courtois, C. and Chamley, H. (1978) Terres rares et minéraux argileux dans le Crétacé et le Cénozoique de la marge atlantique orientale: *C.R. Acad. Sci., Paris* **286D,** 671–674.

Courtois, C., and Hoffert, M. (1977) Distribution des terres rares dans les sédiments du Pacifique Sud-Est: *Bull. Soc. Géol. Fr.* **7,** 1245–1251.

Dasch, E. J. (1969) Strontium isotopes in weathering profiles, deep-sea sediments and sedimentary rocks: *Geochim. Cosmochim. Acta* **33,** 1521–1552.

Desprairies, A., Bonnot-Courtois, C., Jehanno, C., Vernhet, S., and Joron, J. L. (1984) Mineralogy and geochemistry of alteration products in leg 81: in *Initial Reports of the Deep Sea Drilling Project, 81,* D. G. Roberts, D. Schnitker, *et al.,* eds., U.S. Gov. Print. Office, Washington, D.C., 733–742.

Eslinger, E. V. and Savin, S. M. (1973) Oxygen isotope geothermometry of the burial metamorphic rocks of the Precambrian Belt Supergroup, Glacier National Park, Montana: *Geol. Soc. Amer. Bull.* **84,** 2549–2560.

Faure, G. (1982) The marine-strontium geochronometer: in *Numerical Dating in Stratigraphy,* G. S. Odin, ed., Wiley, New York, 73–79.

Goldberg, E. D., Kolde, M., Schmitt, R. A., and Smith, R. H. (1963) Rare earths distribution in the marine environment: *J. Geophys. Res.* **68,** 4209–4217.

Grousset, F. (1983) Sédimentogenèse d'un environnement de dorsale: La ride Açores-Islande au cours du dernier cycle climatique. Origines, vecteurs, flux de particules sédimentaires: Thèse Doc. Sciences, Univ. Bordeaux, Bordeaux, France, 232 pp.

Haskin, L. A., Haskin, M. A., Frey, F. A., and Wildeman, T. R. (1968) Relative and absolute terrestrial abundance of the rare earths: in *Symposium on the Origin and Distribution of the Elements,* L. H. Ahrens, ed., Pergamon, New York, 889–912.

Hess, J., Bender, M. L., and Schilling, J. G. (1986) Evolution of the ratio of strontium 87 to strontium 86 in seawater from Cretaceous to present: *Science* **231,** 979–984.

Hoffert, M. (1980) Les "argiles rouges des grands fonds" dans le Pacifique Centre-Est. Authigenèse, transport, diagenèse: *Mém. Sci. Géol. Strasbourg* **61,** 281 pp.

Hoffert, M., Karpoff, A. M., Clauer, N., Schaaf, A., and Pautot, G. (1978) Néoformations et altérations dans trois faciès volcanosédimentaires du Pacifique Sud: *Oceanol. Acta* **1,** 187–202.

Hogdhal, O. T., Melson, S., and Bowen, V. (1968) Neutron activation analysis of lanthanide elements in sea water: *Adv. Chem.* **73,** 308–325.

Holtzapffel, T. (1983) Origine et évolution des smectites albo-aptiennes et paléogènes du domaine Nord-Atlantique: Thèse 3ème Cycle, Univ. Lille, Lille, 164 pp.

Holtzapffel, T. and Chamley, H. (1986) Les smectites lattées du domaine Atlantique depuis le Jurassique supérieur: Gisement et signification: *Clay Miner.* **21,** 133–148.

Holtzapffel, T., Bonnot-Courtois, C., Chamley, H., and Clauer, N. (1985) Héritage et diagenèse des smectites du domaine sédimentaire nord-atlantique (Paléogène et Crétacé): *Bull. Soc. Géol. Fr.* **8,** 25–34.

Jeans, C. V., Merriman, R. J., Mitchell, J. G., and Bland, D. J. (1982) Volcanic clays in the Cretaceous of southern England and northern Ireland: *Clay Miner.* 17, 105–156.

Kralik, M. (1984) Effects of cation-exchange treatment and acid leaching on the Rb-Sr system of illite from Fithian, Illinois: *Geochim. Cosmochim. Acta* **48,** 527–533.

Leclaire, L. (1974) Hypothèse sur l'origine des silicifications dans les grands bassins océaniques. Le rôle des climats hydrolysants: *Bull. Soc. Géol. Fr.* 7, 214–224.

Louail, J. (1981) La transgression crétacée du Sud du Massif Armoricain. Cénomanien de l'Anjou et du Poitou, Crétacé supérieur de Vendée. Etude stratigraphique, sédimentologique et minéralogique: *Mém. Soc. Géol. Minér. Bretagne* **29,** 300 pp.

Macedo de Freitas, M. H. (1982) Les systèmes isotopiques rubidium-strontium et potassium-argon dans les argiles extraites de sédiments carbonatés. Application à la datation du Protérozoïque sédimentaire du Brésil dans les états de Bahia et Santa Catarina: Thèse Doc. Ing., Univ. L. Pasteur, Strasbourg, France, 119 pp.

Morton, J. P. and Long, L. E. (1980) Rb-Sr dating of Paleozoic glauconite from the Llano region, central Texas: *Geochim. Cosmochim. Acta* **44,** 663–672.

Nathan, Y. and Flexer, A. (1977) Clinoptilolite: Paragenesis and stratigraphy: *Sedimentology* **24,** 845–855.

O'Neil, J. R. (1987) Preservation of H, C and O isotopic ratios in the low-temperature environment: in *Stable Isotope Geochemistry in Low-Temperature Fluids,* T. K. Kyser, ed., *Min. Assoc. Canada, Short Course Handbook* **13,** 85–128.

Piper, D. Z. (1974) Rare earth elements in the sedimentary cycle: A summary: *Chem Geol.* **14,** 285–304.

Savin, S. M. and Epstein, S. (1970a) The oxygen and hydrogen isotope geochemistry of clay minerals: *Geochim. Cosmochim. Acta* **34,** 25–42.

Savin, S. M. and Epstein, S. (1970b) The oxygen and hydrogen isotope geochemistry of ocean sediments and shales: *Geochim. Cosmochim. Acta* **34,** 43–63.

Spirn, R. V. (1965) Rare earth distribution in the marine environment: Ph.D. thesis, Massachusetts Inst. Technol., Cambridge Massachusetts, 165 pp.

Steinberg, M., Holtzapffel, T., Rautureau, M., Clauer, N., Bonnot-Courtois, C., Manoubi, T., and Badaut, D. (1984) Croissance cristalline et homogénéisation chimique de monoparticules argileuses au cours de la diagenèse: *C.R. Acad. Sci., Paris* **299D,** 441–446.

Steinberg, M., Holtzapffel, T., and Rautureau, M. (1987) Characterization of overgrowth structures formed around individual clay particles during early diagenesis: *Clay & Clay Minerals* **35,** 189–195.

Suzuoki, T. and Epstein, S. (1976) Hydrogen isotope fractionation between OH-bearing minerals and water: *Geochim. Cosmochim. Acta* **40,** 1229–1240.

Thellier, C. and Clauer, N. (1989) Strontium isotopic evidence for soil-solution interactions during evaporation experiments: *Chem. Geol.* **73,** 299–306.

Yeh, H. W. and Eslinger, E. V. (1986) Oxygen isotopes and the extent of diagenesis of clay minerals during sedimentation and burial in the sea: *Clays & Clay Minerals* **34,** 403–406.

Yeh, H. W. and Savin, S. M. (1976) The extent of oxygen isotope exchange between clay minerals and sea water: *Geochim. Cosmochim. Acta* **40,** 743–748.

Yeh, H. W. and Savin, S. M. (1977) Mechanism of burial metamorphism of argillaceous sediments. 3. O-isotope evidence: *Geol. Soc. Amer. Bull.* **88,** 1321–1330.

(Received 21 June 1988; accepted 10 May 1989; Ms. 1800)

https://doi.org/10.1346/CCMN.1990.0380105 Published online by Cambridge University Press